SUPPLEMENTAL INFORMATION

SUPPLEMENTAL VIDEOS & FIGURES

Videos 1–4. Three-dimensional reconstructions, related to Figure 1. 1st telogen (video 1), anagen (video 2), catagen (video 3), and 2nd telogen (video 4).

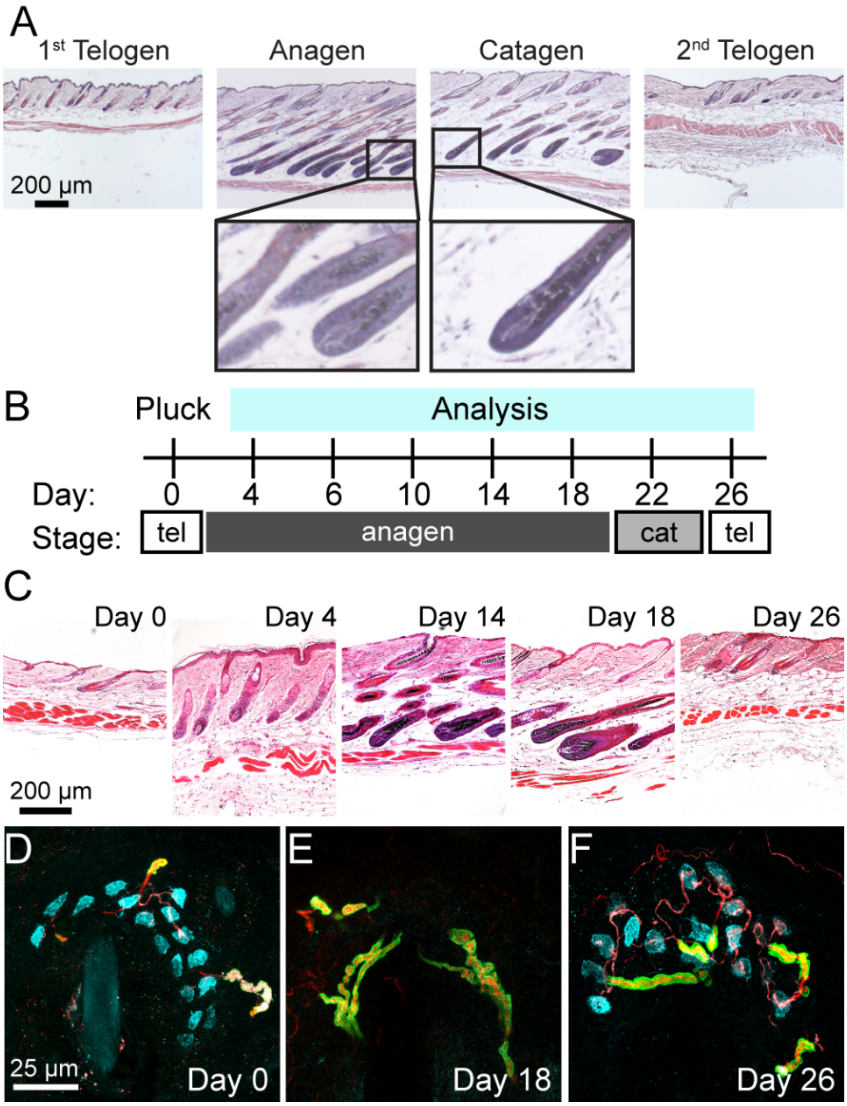

Figure S1. The mouse hair cycle, related to Figures 1 & 2.
(**A**) Stages of the first spontaneous hair cycle (related to **Figures 1B–I & 2A–C**). Hemotoxylin and eosin (H&E)-stained skin sections show hair follicles in first telogen (P23), anagen (anagen VI, P35), catagen (catagen I, P44) and second telogen (P66). Boxed regions are shown below at increased magnification. (**B**) Experimental paradigm for plucking-induced hair cycles (related to **Figures 1J, K**). Vertical lines denote time points for collecting specimens (*N*=3–4 mice per group). (**C**) H&E-stained skin sections from 0 (unplucked), 4, 14, 18, and 26 days after plucking. (**D–F**) Representative axial projections of whole-mount touch-dome innervation before plucking (Day 0) or at the indicated days post-plucking. K8: cyan, NFH: red, MBP: green.

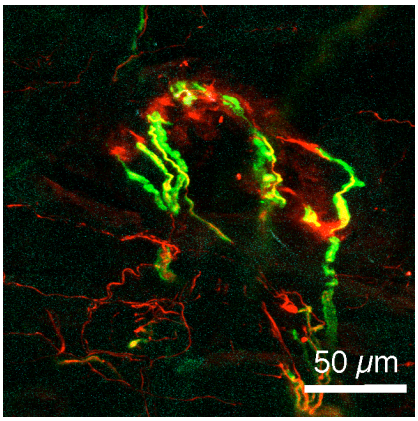

Figure S2. Anagen touch-dome afferents display diffuse terminal NFH+-immunoreactivity, related to Figure 1B.
An example projection from a touch-dome afferent that terminated in bright NFH+ regions more distal to myelin end-points. K8-positive Merkel cells were not detected in this touch dome. K8: cyan, NFH: red, MBP: green.

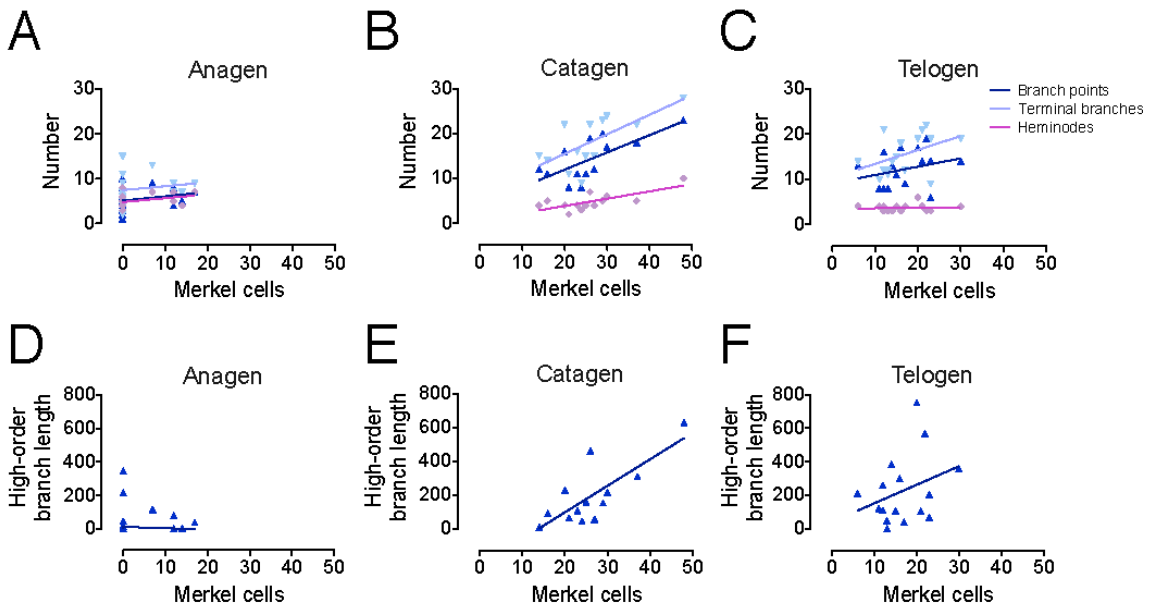

Figure S3. Unmeylinated neurites account for most of the afferent remodeling in the hair cycle, related to Figures 1D–I.
(**A–C**) The number of branch points (blue), terminal branches (light blue) and heminodes (magenta) plotted against the number of K8+ Merkel cells in a given touch dome during spontaneous anagen (**A**), catagen (**B**) and telogen (**C**). Linear regressions revealed a significant correlation with a non-zero slope only for parameters in catagen (**B**; R^2=0.47–0.53, *P*=0.005–0.01, Pearson's correlation). (**D–F**) The total length of all branches fifth order and above plotted versus number of K8+-Merkel cells in anagen (**D**), catagen (**E**) and telogen (**F**). This measure correlated with Merkel-cell number only in catagen (**E**; R^2=0.6, *P*=0.002, Pearson's correlation; *N*=3–4 animals and 13–19 touch domes per group).

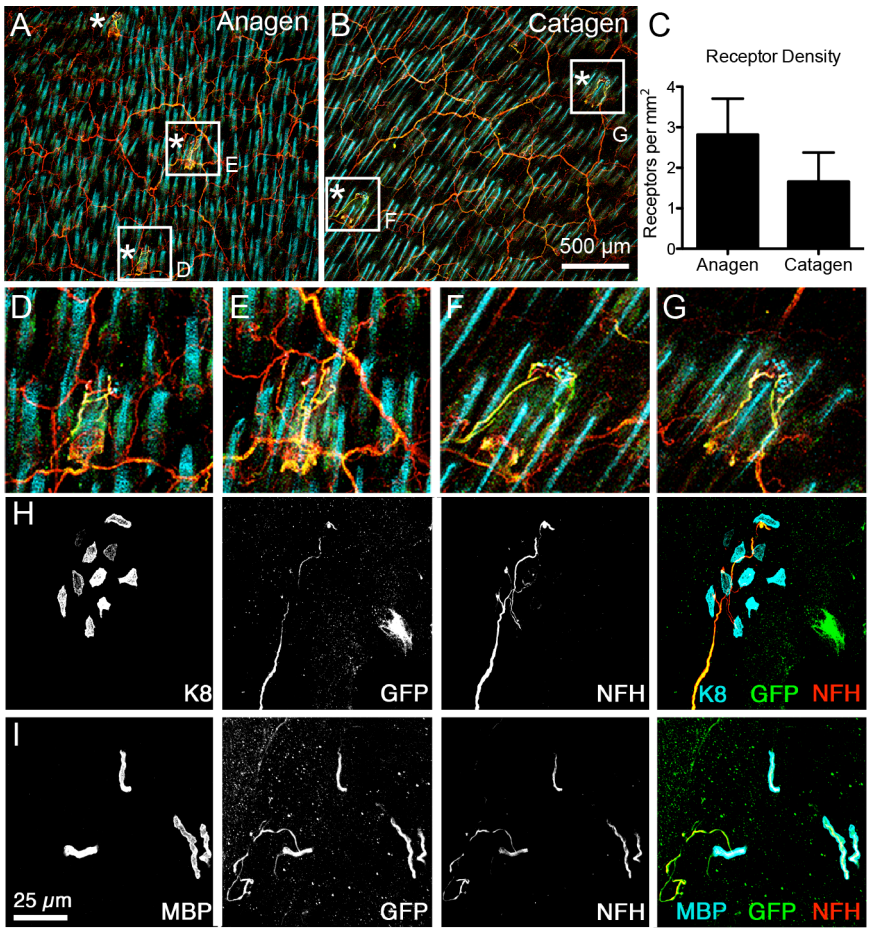

Figure S4. Additional analysis of anagen afferents, related to Figures 2 & 4.

(**A–B**) Myelinated afferent density increases modestly in anagen (related to **Figures 2D-G)**. Representative axial projections of skin specimens labeled with antibodies against NFH (red), MBP (green) and K8 (cyan) during spontaneous anagen (**A**) and catagen (**B**; scale bar in **B** applies to **A**). Asterisks denote myelinated branches that approach the epidermis and were scored as touch-dome innervation. Note the two Merkel-cell clusters in catagen whereas none was observed in anagen. (**C**) Quantification of end-organ density (mean±SD; P=0.005, two-tailed Student's t test, N=9–11 fields from 2–3 animals). (**D–E**) Magnified from insets in **A**. (**F–G**) magnified insets from **B**. **(H–I)** Piezo2 is expressed throughout touch-dome afferents in anagen (related to **Figure 4)**. Axial projections from anagen touch domes in *Piezo2-gfp* mice. Antibodies were used to visualize the antigens indicated by panel labels. A typical arbor containing Merkel cells (**H**) and a simplified arbor (**I**) are shown. Scale bar in **I** applies also to **H**.

SUPPLEMENTAL TABLES

Table S1. Response properties of Aβ afferents recorded during unbiased mechanical survey

Fiber type	Conduction velocity (m/s)				von Frey threshold (mN)				# afferents	
	Ana		Tel		Ana		Tel		Ana	Tel
	mean	*SD*	*mean*	*SD*	*median*	*range*	*median*	*range*	*total: 20*	*total: 19*
Aβ RA	11.7	1.6	12.8	3.1	0.39	0.08–98.0	0.3	0.2–0.69	9	6
Aβ SAI	11.5	0.0	12.6	2.4	0.08	N/A	0.08	0.08–0.08	1	5
Aβ other SA	13.3	3.0	11.2	1.6	0.08	0.08–0.2	0.14	0.08–3.92	10	8

Table S1. Response properties of Aβ afferents recorded during unbiased mechanical searches in anagen (Ana) and telogen (Tel).
Conduction velocity and von Frey thresholds are indicated. Rapidly adapting (RA) responses produced spike trains only during dynamic stimulation. SAI afferents were classified as noted in *Methods*. Aβ other SA had a sustained reponse patterns but did not otherwise meet the classification criteria for SAI responses.

	KS test normal?	P value	Skewness	*N*=
Boltzmann slope - dynamic				
Ana	No	< 0.0001	3.1	13
Cat	Yes	0.08	0.68	8
Tel	Yes	> 0.10	0.38	8
Boltzmann slope - static				
Ana	No	0.005	2.28	11
Cat	No	0.01	1.61	7
Tel	Yes	> 0.10	1.37	8
Boltzmann F50 - dynamic				
Ana	No	< 0.0001	3.25	13
Cat	Yes	0.06	0.97	8
Tel	Yes	> 0.10	-0.59	8
Boltzmann F50 - static				
Ana	No	0.002	2.83	11
Cat	No	0.006	2	7
Tel	Yes	0.09	1.97	8
Force threshold				
Ana	No	< 0.0001	2.17	13
Cat	No	0.01	1.37	11
Tel	No	0.01	1.4	8

Table S2. Normality and skewness values for SAI response properties in targeted recordings.
Results from Kolmogorov-Smirnov (KS) test of normality are shown, with "yes" indicating that data follow a normal distribution (P>0.05). Skewness values represent symmetry of the data, with zero indicating perfect symmetry and positive values indicating rightward skew.

ONLINE MATERIALS AND METHODS

Animals

Animal use was conducted according to guidelines from the National Institutes of Health's Guide for the Care and Use of Laboratory Animals and was approved by the Institutional Animal Care and Use Committee of Columbia University Medical Center. Adult female mice were used for all experiments. C57BL/6 mice were analyzed unless noted. Postnatal (P) ages are indicated in methods or figure legends. Proximal hindlimb skin specimens were analyzed, except where back skin is indicated.

Anatomical analysis of Merkel-cell afferents over the hair cycle

To investigate afferents over the first spontaneous hair cycle, skin specimens were collected from *Atoh1/nGFP* (**Figure 1B–I**; MGI: Tg(Atoh1-GFP)1Jejo) or C57BL/6 mice (**Figure 2A–C, E & G**; P24–70). Some morphometric data collected in second telogen were previously reported (Lesniak *et al.*, 2014). Based on skin pigmentation, these ages were determined to span first telogen through second telogen in both the proximal hindlimb and back skin, which have slightly different temporal progressions through the hair cycle. Hair cycles were verified post hoc by histological staging of follicles as described below.

To analyze induced hair cycles, C57BL/6 or $Atoh1^{A1GFP/A1GFP}$ (MGI: $Atoh1^{tm4.1Hzo}$) mice (9–10 weeks old) were anesthetized with 5% Isoflurane and maintained at 2–3% using a vaporizer according to approved protocols. Hair shafts were plucked in a 2 cm^2 patch located on the proximal hindlimb. For analysis of temporal dynamics (**Figure 1J–K**), skin specimens were collected 4–26 days post-plucking (N=3-4 mice per time point and ≥5 touch domes per mouse). For analysis of Atoh1-GFP expression (**Figure 2D & F)**, hindlimb skin specimens were collected 18 or 22 days after plucking (N= 8–10 touch domes per mouse and 2–3 mice per time point).

Assessment of hair-cycle stage

Natural hair cycle stages were assessed based on skin pigmentation and animal age according to published methods (Muller-Rover *et al.*, 2001). As the onset of spontaneous hair cycling is variable, hair-cycle stages were typically confirmed post hoc histologically using areas of skin adjacent to whole-mount specimens or recorded receptive fields. Specimens were fixed overnight in 4% PFA at 4°C, transferred into 70% ethanol, paraffin-embedded, sectioned at 5 μm and stained with hematoxylin and eosin using standard protocols. A total of 25–105 follicles from ≥3 sections per specimen were matched to hair-cycle stages as described (Muller-Rover *et al.*, 2001), and the sample was classified according to the follicle stage that described ≥70% of follicles. Specimens that fell between two cycle stages were excluded from further analyses. Late anagen was defined as anagen IV-VI.

Immunohistochemistry and confocal microscopy

Skin was depilated (Surgi-cream), tape-stripped to remove the stratum corneum and dissected from the proximal hind limb or back. The hindlimb location was chosen to match the site of electrophysiological recordings in *ex vivo* skin-saphenous nerve preparations, and the dorsal location was chosen for comparison with previous literature and consistency with behavioral studies. Whole-mount immunohistochemistry was performed as previously described (Lesniak *et al.*, 2014). Briefly, tissue was fixed in 4% paraformaldehyde (PFA) overnight, washed in 0.03% triton-X PBS (PBST) and incubated in primary antibody for 72–96 h at 4°C. Primary antibodies used were: rat anti-K8 (Developmental Studies Hybridoma Bank; TROMA-I), chicken anti-NFH (Abcam; ab4680), rabbit anti-NFH (Abcam; ab8135), rabbit anti-MBP (Abcam; ab40390), rabbit anti-VGLUT2 (Synaptic Systems, 135402), and chicken anti-GFP (Abcam; ab129070). After 5-10 h of washes in PBST, samples were incubated for 48 h at 4°C in secondary antibodies: goat AlexaFluor-conjugated antibodies (Invitrogen) directed against rat (Alexafluor 594; A11007), chicken (Alexafluor 647; A21449) or rabbit (Alexafluor 488; A11008) IgG. After staining, tissue was dehydrated progressively in 25-100% methanol and cleared using a 2:1 benzyl benzoate/benzyl alcohol solution. Specimens were imaged in three dimensions (0.5–1 μm axial step sizes) on a Zeiss Exciter confocal microscope equipped with 20X, 0.8 NA or 40X, 1.3 NA objective lenses.

Experimenters could not be blinded to hair cycle stage during experiments because of obvious differences in skin color, thickness, and follicle sizes across hair cycle stages. Quantification was performed in unprocessed axial stacks. For publication, representative images were cropped to regions of interest and output levels were linearly adjusted in photoshop to ensure the histogram filled the dynamic range. Gamma was not changed.

Three-dimensional reconstructions

Confocal image stacks were imported into Neurolucida (MBF Bioscience) and traced in three dimensions. Tracing data were analyzed using Neurolucida Explorer branching analysis tools. Images were prepared for publication in ImageJ (Schneider *et al.*, 2012) or Photoshop (Adobe). Three-dimensional reconstruction videos were created with the 3D-visualization tool in Neurolucida. We traced Merkel-cell afferents from the neural plexus to the unmyelinated branches, termed neurites, in the epidermis. Five branching parameters were analyzed over the entirety of the afferent: terminal branches, defined as the most distal branches; branch points; highest branch order, which reflects the number of sequential branch points (an unbranched afferent has a highest branch order of 1, while an afferent that branches once is second order), total afferent length, and number of heminodes, defined as the end-points of MBP staining.
To quantify lengths of unmyelinated arbors, high-order branches were defined as fifth-order and above because myelin end-points most often occured on fourth-order branches in telogen (Lesniak *et al.*, 2014).

Electrophysiology

Extracellular recordings from mouse *ex vivo* skin-saphenous nerve preparations were performed as previously described (Maricich *et al.*, 2009; Maksimovic *et al.*, 2014). Spike discrimination and data analysis was performed in MATLAB. Because of changes in skin pigmentation over the hair cycle, experimenters could not be blinded to hair-cycle stage during recordings; however, electrophysiological data were blinded for subsequent analysis and curve fitting.

Female C57BL/6J mice during first anagen, second catagen and second telogen (P30–87) were used. Hair-cycle stage was confirmed post hoc by histology as described above. To estimate the proportion of afferents that produced SAI responses in anagen versus telogen, an unbiased survey of Aβ afferents was performed using a mechanical search strategy as previously described (Maricich *et al.*, 2009). For targeted recordings from touch-dome afferents, a published mechanical search strategy was used to locate units with Aβ conduction velocities (CV≥9 m/s) that responded selectively to touch-dome indentation (Maksimovic *et al.*, 2014).

SAI responses were classified according to criteria of Iggo & Muir (Iggo and Muir, 1969): 1) Aβ conduction velocity, 2) sustained firing with irregular interspike intervals; 3) punctate receptive fields restricted to one or more touch domes, 4) unresponsive to guard-hair movement unless it compressed a touch dome. In addition to afferents that produced canonical SAI responses, we observed touch-dome afferents that responded to guard-hair wiggle (Y.B., unpublished observations). These responses were not analyzed further because the end-organ structure of these afferents has not been elucidated.

Mechanical stimuli were delivered via a ceramic cylindrical probe (1.5-mm tip diameter) mounted on a custom indenter (Wellnitz *et al.*, 2010). Ramp-and-hold stimuli were applied in a randomized order. Five-second hold durations were used throughout. Typically, 2–3 presentations were performed at each stimulus magnitude and firing rates were averaged for curve fitting. The skin's reactive force was monitored with a load cell mounted on the indenter; mean force levels for the late hold phase (2–4.5 s after the probe reached the commanded stimulus) are reported. Instantaneous firing rates (as in **Figure 4D–F**) were calculated as reciprocals of inter-spike intervals. Dynamic firing rate was defined as the peak instantaneous firing rate observed during stimulus ramp (*i.e.*, the time period of probe movement). Static firing rate was calculated as the mean of the instantaneous firing rates during the late-hold phase, which excludes a period of rapid adaption that follows the dynamic phase of the SAI response. To compare dynamic and static firing rates across populations of afferents (**Figure 4J**), we calculated the maximal dynamic and static firing rates for each unit at the stimulus magnitude that elicited most robust firing.

Tape response test

Tactile behavior driven by receptors in hairy skin was assessed using a modified version of the tape response test (Bouet *et al.*, 2009; Ranade *et al.*, 2014) which was chosen to preferentially interrogate the contribution of SA afferents. The tape response test delivers a sustained pressure on the hairy skin, rather than stroking or air puff, which maximally activates RA receptors (Garrison *et al.*, 2012; Bai *et al.*, 2015). Female C57BL/6 mice (age P35–P54) were tested. Mice were anesthetized with isoflurane, shaved, and hair was removed from the lower back with depilatory cream to further minimize the contribution of RA afferents (Surgi-cream). Mice were individually placed in clean cages, allowed to acclimate for 30 min, and then stickers (9.5 mm in diameter; Microtube Tough-Spots, 9175-1100) were placed on the depilated skin. Catch trials, in which a mouse was touched with the non-adhesive side of the sticker, were pseudo-randomly interspersed with stimulus trials to evaluate whether mouse handling was used as a cue for sticker detection. Two sessions with six trials each were performed in anagen and second telogen. Sessions were videotaped and responses were manually scored for 5 min after trial initiation post hoc with VLC media player.

Detection of the sticker was defined as when the mouse reared onto its hind legs and touched the sticker with either the nose or forepaw. The average latency to sticker detection across all hit trials was analyzed in Matlab and is reported for each animal. Two cohorts of 10 mice each were tested.

Simulations of afferent plasticity

The goal of computational simulations was to test whether a set of simple rules can account for the observed arbor remodeling over a natural hair cycle. Simulations were custom programmed in Python to evaluate policies of Merkel-cell and heminode addition and removal. Each of the transitions between hair-cycle stages were modeled as a separate simulation. Within each simulation, there were a number of iterations where Merkel cells and/or heminodes could be added or removed according to four policies, which were informed by morphometric data (**Figure 1**). Thirty end organs in first telogen were created by an auto-generation method based on randomly chosen Merkel-cell and heminode numbers bounded by experimentally observed distributions in first telogen (**Figure 1D, I**). Merkel cells were randomly distributed amoung heminodes to produce Merkel-cell clusters of different sizes, as found in mouse touch-dome afferents (Lesniak *et al.*, 2014).

Each end organ then went through a complete hair cycle according to four policies (**Figure 3A**). From first telogen to anagen, Merkel cells were reduced to nearly zero using a proportional removal policy (Policy 1). Specifically, Merkel cells were removed until the population mean and variance matched that of the biological data. Merkel cells were more likely to be eliminated from heminodes with large Merkel-cell clusters. To transition from anagen to catagen, heminodes lacking Merkel cells were pruned by an average of two (Policy 4). This simulation was repeated until the distributions of heminode numbers matched the mean and variance of the biological data. Merkel cells were then randomly added to remaining heminodes (Policy 2). From catagen to second telogen, heminodes were reduced again by removing heminodes with the smallest numbers of Merkel cells (Policy 4). Finally, we employed a procedure aimed at decreasing the variance as observed in the distributions of Merkel cells and heminodes in second telogen (**Figure 1D, I**). For this step, we employed a series of specific interventions, as opposed to the general policies regarding probabilistic addition and removal of Merkel cells and heminodes detailed above. In catagen end organs, one heminode was deleted if there were more than four heminodes, but one heminode was added if there were fewer than three heminodes. Similarly, if an end organ had fewer Merkel cells than the mean number observed in second telogen, five Merkel cells were added, and if the end organ had more Merkel cells than the mean, five Merkel cells were deleted (Policy 3). The deletion of Merkel cells at this step was proportional to cluster size as in Policy 1, so deletions were more likely to occur in large Merkel-cell clusters.

Overall, the model relies on several assumptions: 1) observed mean values in the hind limb spontaneous hair cycle dataset are accurate enough to make logical policies, 2) heminodes with the smallest number of Merkel cells are most likely to be removed, 3) Merkel cells are randomly added to heminodes. The model produced a set of frequency histograms for the number of Merkel cells and heminodes per touch dome for each stage of the hair cycle (**Figure 3**).

Data Analysis and Statistics

Statistical analyses were performed with Prism 5 (Graphpad). For parametric data with three or more groups, one-way ANOVAs were followed by Tukey's *post hoc* analysis for between-group comparisons. Unpaired, non-parametric data were analyzed using the Kruskal-Wallis test with Dunn's *post hoc* comparison. Paired data were compared with Wilcoxon matched-pairs signed rank test. Student's two-tailed *t* test was used to compare means of two normally distributed groups. Categorical behavioral data were compared using the two-tailed Fisher's exact test. Linear regressions were performed in Prism and Pearson's correlation values were assessed based on these fits. The normality of population data was assessed using the Kolmogorov-Smirnov test with Dallal-Wilkinson-Lilliefors *P* values, with $P \leq 0.05$ indicating non-normality. For electrophysiology data, datasets that were non-normal were log transformed ($Y=\log(Y)$) before testing for outliers using Grubb's test, which utilized the extreme studentized deviate method. One outlier was detected and was excluded from the dataset.

Force-firing rate relations (**Figure 4G–I**) were analyzed by plotting the firing rate averaged from multiple stimulus presentations against mean static force. Curves were fit with a Boltzmann function:

$$Firing\ rate\ (F) = \frac{Plateau}{1 + \exp\left(\frac{F_{50} - F}{s}\right)}$$

where *Plateau* denotes peak firing rate, F is a given force, F_{50} is force that produces half-maximal amplitude of peak firing rate, and s denotes a slope function that is inversely proportional to the unit's sensitivity. Fits were constrained through zero to reflect the lack of spontaneous firing in SAI responses. Ambiguous Boltzmann fits were excluded from further analysis. Of 33 touch-dome units, 26 were fit in the static phase and 29 were fit in the dynamic phase.